ACS APPLIED MATERIALS & INTERFACES

Research Article

www.acsami.org

Thermoelectric Performance of $SrTiO_3$ Enhanced by Nanostructuring—Self-Assembled Particulate Film of Nanocubes

Feng Dang,*[,†,‡] Chunlei Wan,*[,†,‡] Nam-Hee Park,[†,‡] Kazuki Tsuruta,[†] Won-Seon Seo,[§] and Kunihito Koumoto*[,†,‡]

[†]Graduate School of Engineering, Nagoya University, Nagoya 464-8603, Japan

[‡]CREST, Japan Science and Technology Agency, Tokyo 102-0075, Japan

[§]Korea Institute of Ceramic Engineering & Technology, Seoul 153-801, Korea

Supporting Information

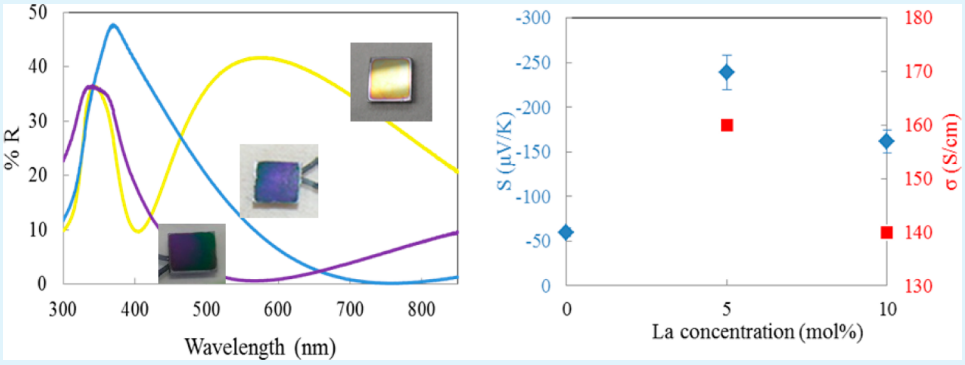

ABSTRACT: Self-assembled particulate films with a uniform structure over a large area were prepared from La-$SrTiO_3$ nanocubes for thermoelectric applications. UV irradiation was used to assist the formation of particulate film for decomposition of the organic phase in situ to obtain a mechanically robust structure at high temperature. The thermoelectric properties of the particulate film were measured after calcination at 1000 °C under a reductive atmosphere (Ar/H_2 = 60/40). A Seebeck coefficient of $S = -239 \pm 24$ μV/K, electrical conductivity of $\sigma = 160 \pm 5$ S/cm, and thermal conductivity of $\kappa \approx 1.5$ W/mK were obtained for a self-assembled particulate film (La: 5%) corresponding to a ZT value of 0.2 at room temperature, which exceeded that of a La-$SrTiO_3$ single crystal with similar composition.

KEYWORDS: *$SrTiO_3$, nanocubes, self-assembly, particulate film, thermoelectric, La doping*

INTRODUCTION

Strontium titanate ($SrTiO_3$, abbreviated as STO), is a perovskite-type material, with cubic crystal structure and band gap of 3.2 eV due to highly populated O-p- and Ti-e_{2g}-states.[1−3] Heavily doped STO is considered a promising n-type oxide semiconductor because it exhibits a high Seebeck coefficient (S) owing to a large effective electron mass (m^* = 6−15 m_o).[4−15]

Our previous work on La and Nb doping of STO featured the development of thermoelectric properties of STO.[4−11] La-doped STO single crystal had a ZT value of 0.08 at 300 K with an electrical conductivity of σ = 1000 S/cm and Seebeck coefficient of $S = -150$ μV/K.[4] A ZT value of 0.37 at 1000 K was measured for Nb-doped STO epitaxial films.[5] Furthermore, we found that Nb-STO/STO superlattices exhibited a massive Seebeck coefficient resulting in a ZT value of 2.4 at 300 K for a one-unit-cell-thick Nb-STO layer owing to formation of a two-dimensional electron gas (2DEG).[6]

However, a large thermal conductivity of κ = 11 W/mK limits enhancement of the ZT value of bulk STO. Our previous work has demonstrated that smaller crystal grain size lowers the thermal conductivity of a bulk polycrystalline ceramic significantly because of enhanced phonon scattering at grain boundaries.[9] An analysis assuming Kapitza resistance at grain boundaries with 10 nm grain sizes suggested a thermal conductivity of 2 W/mK at 300 K may be achievable in STO nanoceramics.[9] However, porous or nano-structure always decrease the crystallinity, which results in the decrease of Seebeck coefficient or electric conductivity. Self-assembled structure of nanoparticles with good crystallinity provide a possibility to realize the low thermal conductivity with high Seebeck coefficient and electric conductivity. In this work, a self-assembled particulate film of La-STO nanocubes was prepared to realize a low thermal conductivity with high Seebeck coefficient and electric conductivity.

Received: July 31, 2013
Accepted: October 3, 2013
Published: October 3, 2013

Many techniques, such as dip-coating, layer by layer processing, slow evaporation, and Langmuir−Blodgett methods, have been developed to prepare self-assembled structures from nanoparticles.[16−21] We have prepared a series of self-assembled structures from CeO_2, $SrTiO_3$, and $BaTiO_3$ nanocubes using different methods.[19−21] For preparation of a self-assembled structure, organic phases such as surfactant or polymer molecules are needed to ensure the dispersibility of the nanoparticles in solution. However, the existence of the organic phase limits the application of the system at high temperatures. For thermoelectric applications, the nanocubes must have good contact with each other and the self-assembled structure must be stable to high temperature. For STO, its electrical conductivity must also be maintained after heat treatment at 1000 °C under a reducing atmosphere.

In the present work, we introduce the preparation of a self-assembled particulate film of monodisperse La-STO nanocubes with mechanically robust structure at high temperature. UV irradiation was used to prepare self-assembled particulate films by in situ decomposition of adsorbed surfactant molecules. Uniform structure and structure colors were produced in the self-assembled particulate film of La-STO nanocubes. The self-assembly structure of the nanocubes was preserved after heat treatment at 1000 °C under a reducing atmosphere, and its ZT at 300 K exceeded that of a single crystal with a similar composition.

EXPERIMENTAL SECTION

Bis(ammonium lactate) titanium dihydroxide (TALH) (0.05 mol/L, Ba:Ti = 1:1) was added into an aqueous solution of $Sr(OH)_2$ and $La(OH)_3$ (24 mL, 0−10%). A 5 mol/L aqueous NaOH solution was added to the reaction mixture with mechanical stirring, to produce a NaOH concentration of 0.8 mol/L. The reaction mixture was transferred to a 50 mL autoclave, and then hydrazine and oleic acid (OLA) (Sr:OLA:hydrazine = 1:4:8) were added into the solution. The sealed autoclave was heated at 200 °C for 48 h and then cooled to room temperature. After the synthesis, the nanocubes were centrifuged at 3000 rpm, washed twice with ethanol, and then dispersed into toluene. The dispersed La-STO nanocubes were dropped on a Si (100) substrate (0.5 × 0.5 cm^2) at room temperature, and then toluene was evaporated under UV irradiation (Photo Surface Processor PL21−200, Sen Lights Corp.) in air for 30 min to prepare a particulate film. The self-assembled particulate film was calcined at 1000 °C under a reducing atmosphere (Ar/H_2 = 60/40) for 2 h to obtain thermoelectric properties. In comparison, the self-assembled films of nanocubes were also prepared in vacuum (3 kPa) as shown in Supporting Information Figure S3b.

The nanocubes and the self-assembled particulate films were characterized by X-ray diffraction (XRD, Rigaku Rint 2100), scanning electron microscopy (SEM, JEOL JSM-7500FA), transmission electron microscopy (TEM, JEOL JEM-4010), dynamic light scattering (DLS, ELSZ-1000S), atomic force microscopy (AFM), and Fourier transform infrared spectroscopy (FT-IR) methods (Perkin-Elmer Spectrum). The reflectance spectra of the self-assembled particulate films were measured by ultraviolet and visible spectrophotometric lifht (JASCO V-650). The Seebeck coefficient and $I-V$ curve of the films were measured using a homemade measurement system (Figure 3c,d). Electrical conductivity of the films was measured by using the van der Pauw method (Supporting Information Figure S5). The thermal conductivity of the films was measured using a nanosecond light pulse heating thermoreflectance method (PicoTherm NanoTR).

RESULTS AND DISCUSSION

The La-STO nanocubes were synthesized using TALH as a Ti precursor in aqueous solution.[22,23] The selection of the 6-coordinated Ti precursor (TALH) encouraged oleic acid (OLA) to selectively adsorb on the Sr rich (100) face of STO encouraging the formation of nanocubes.[23] Monodisperse La-STO nanocubes (La: 5%) with a size of ca. 15 nm were obtained as shown in the TEM and HRTEM images (Supporting Information Figure S1a,b). The nanocube size increased at higher La concentrations (Supporting Information Figure S1d,e). The La-STO nanocubes were dispersed into toluene (Supporting Information Figure S1a), and the DLS result of the dispersion indicated particle sizes of 23−30 nm (Supporting Information Figure S1c).

Self-assembled particulate films of La-STO nanocubes were prepared by evaporating toluene on a Si substrate under UV irradiation for 30 min as shown in Figure 1a. It is worth noting

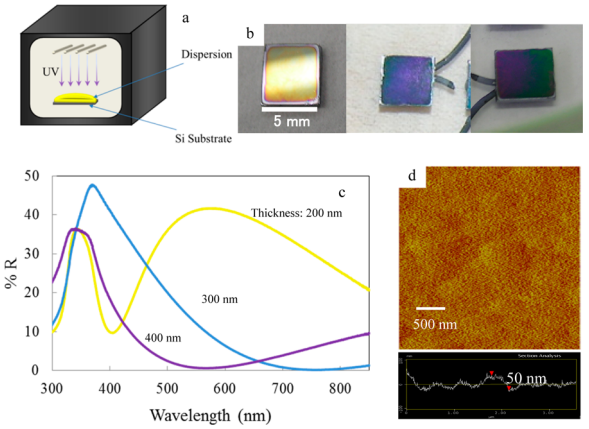

Figure 1. (a) Illustration of the preparation of the self-assembled particulate film; (b) photograph of the self-assembled film; (c) reflectance spectra and (d) AFM image of the self-assembled particulate film.

that a uniform particulate film could not be obtained without the UV irradiation (Supporting Information Figure S2). Structure colors were observed from the self-assembled films as shown in Figure 1b. The films of La-STO nanocubes appeared yellow, blue, and purple, corresponding to different thickness. The reflectance spectra of the particulate film with different structure colors mainly concentrated in the UV bands as shown in Figure 1c. It is suggest that the reflectance spectra near UV bands are mainly attributed to the particle size of nanocubes and indicate the uniform structure of the prepared particulate films. Smooth surface with a roughness smaller than 50 nm was obtained for the particulate film as shown in Figure 1d. SEM images (Figure 2a,b) also indicated the formation of a highly uniform particulate film with no cracks. All the cube faces were 100 planes as shown in Figure 2b. Only the 200 peak was identified in the XRD pattern of the self-assembled film (Figure 2d). It firmly indicates that the nanocubes aggregated epitaxially with each other. The thickness of the observed particulate film (La: 5%) was about 500 nm (Figure 2c). Supposing that the nanocubes have uniform size and the self-assembled particulate film has the perfect layer structure, the relative density of the self-assembled particulate film was estimated through counting the number of nanocubes in a given area (Figure 2b). The relative density (packing ratio) of the self-assembled particulate film was estimated to be 78%. The packing ratio (78%) of nanocubes in the self-assembled particulate film exceeded that (68%) of a body-centered cubic

dx.doi.org/10.1021/am403112n | ACS Appl. Mater. Interfaces 2013, 5, 10933−10937

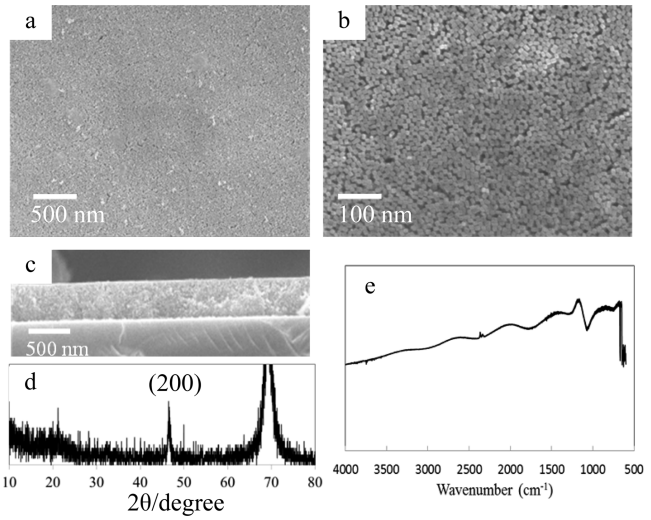

Figure 2. (a–c) SEM images, (d) XRD patter,n and (e) FT-IR spectra of the self-assembled particulate film of La-STO (La 5%).

and were slightly larger than that (74%) of a face-centered cubic (FCC) structure composed of spherical particles.

Dip-coating, slow evaporation, electric deposition, and Langmuir–Blodgett methods are usually used for the preparation of self-assembled films of nanoparticles. However, these methods are not suitable for preparation of films of nanocubes smaller than 20 nm over a large area with uniform structure. The method we describe allowed the successful formation of a self-assembled film of La-STO nanocubes over a large area. UV irradiation was found essential for the formation of a self-assembled film with uniform structure. Figure 2e shows the FT-IR spectra of the self-assembled particulate films. Peaks corresponding to OLA and other organic phases were not detected. The UV irradiation likely caused decomposition of the organic phases (oleic acid and residual toluene), facilitating assembly of the nanocubes into a self-assembled film. The in situ decomposition of the organic phase resulted in good contacts between nanocubes and a mechanically robust self-assembled particulate film. Although close-packed structures of nanocubes were obtained for self-assembled films prepared under vacuum, large cracks were observed after the decomposition of the organic phase (Supporting Information Figure S3).

The as-prepared La-STO nanocubes were electrically insulating. To improve electrical conductivity, the self-assembled particulate film was calcined under a reducing atmosphere to generate conduction electrons through oxygen release. In this work, the particulate film was calcined at 1000 °C under an Ar/H_2 atmosphere with a H_2 concentration of 40%. After calcination, the structure of the self-assembled particulate film was maintained showing formation of grain boundaries with little growth of grains during calcination (Supporting Information Figure S4). However, as shown in Figure 3a, cracks of ca. 500 nm in length were introduced possibly by changes in local density during calcination, while the size of nanocubes did not change during calcination. Diffraction peaks of 110, 111, and 210 planes were identified from the XRD patterns (Figure 3b) of the particulate film, indicating that some nanocubes deviated from [100] orientation during calcination.

The Seebeck coefficient (S), electrical conductivity (σ), and thermal conductivity (k) of the calcined self-assembled particulate film were measured at room temperature. A Seebeck coefficient, S, of -239 ± 24 μV/K was measured for the particulate film of La-STO nanocubes with La concentration of 5% as shown in Figure 3c, and the electrical conductivity, σ, was measured by using a van der Pauw method as 160 ± 5 S/cm.

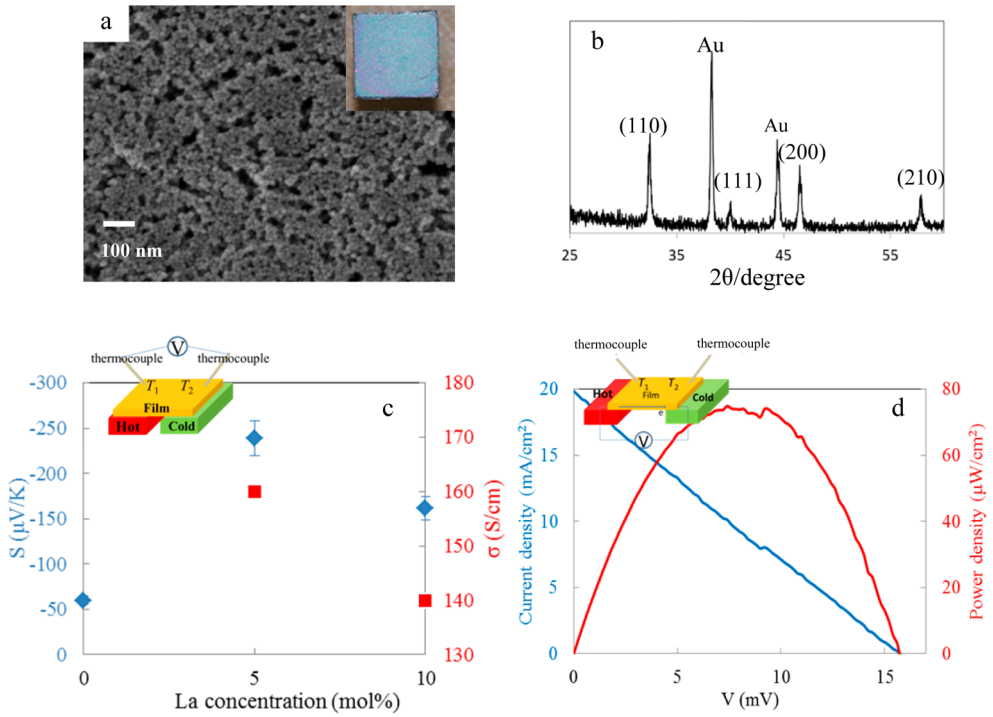

Figure 3. (a) SEM image and photograph and (b) XRD pattern obtained after calcination (La 5%); (c) Seebeck coefficients measured for the self-assembled particulate films; (d) I–V and power density curves of the self-assembled particulate film (La 5%) with a temperature difference of 20 K.

dx.doi.org/10.1021/am403112n | ACS Appl. Mater. Interfaces 2013, 5, 10933–10937

On the other hand, the particulate film of pure STO nanocubes was still electrically insulating. A very low thermal conductivity, κ, of 1.5 W/mK was obtained for the particulate films, which is only 14% of that of STO single crystal. The ZT value ($S^2\sigma/\kappa$) of the self-assembled particulate film was estimated to be 0.2 at 300 K, which is far larger than that of the La-STO single crystal (ZT = 0.08) with a similar composition.[4]

The self-assembled particulate films feature two unique properties associated with the increased number of grain boundaries, which may enhance thermoelectric performance: an energy filtering effect can occur at grain boundaries, enhancing the Seebeck coefficient; and phonon scattering at grain boundaries is enhanced, which can reduce the thermal conductivity significantly. Figure 4 shows the Log |S|−log σ plot

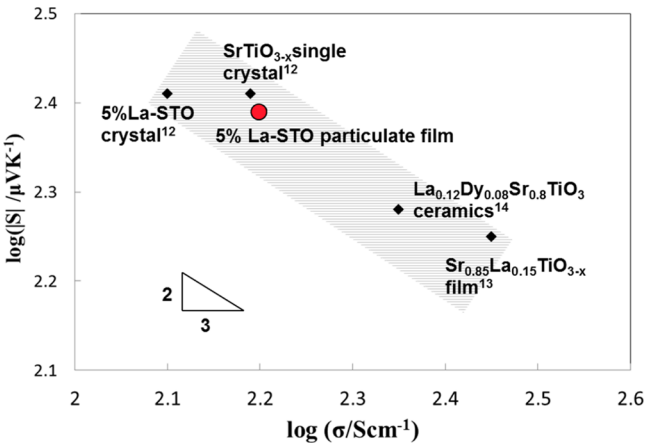

Figure 4. Log |S|−log σ plot for La-STO summarized from the data reported in the literature (refs 12−14).

for La-STO summarized from data reported in the literature.[12−14] The plot for the La-STO self-assembled film obtained in this study is shown for comparison. The Seebeck coefficient of a degenerate semiconductor and its electrical conductivity, respectively, are expressed in general as follows:

$$S = (8\pi^2 k_B{}^2/3eh^2)m^* T(\pi/n)^{2/3} \quad (1)$$

$$\sigma = ne\mu \quad (2)$$

where k_B is Boltzmann constant, h the Planck constant, e the electron charge, m^* the carrier effective mass, T the absolute temperature, n the carrier concentration, and μ the carrier mobility. The relationship between the Seebeck coefficient and electrical conductivity can be deduced from the above equations as $S \propto \sigma^{-2/3}$. Figure 4 illustrates that the literature data are in good agreement with this relationship, and the plot for the particulate film of this study obeys the relationship. This result firmly indicates that electronic conduction in the self-assembled particulate film takes place by a mechanism similar to other La-STO crystals. It can be concluded that the large Seebeck coefficient (−239 ± 24 μV/K) of the self-assembled film is not because of an energy filtering effect but can be attributed only to a low electrical conductivity. The high ZT value of 0.2 at 300 K that was measured in the self-assembled particulate film is therefore attributed to its low thermal conductivity.

Lower thermal conductivity in bulk polycrystalline STO with smaller grain size was identified in our previous work.[9] Through enhanced phonon scattering at grain boundaries, the thermal conductivity would decrease to 2 W/mK when the grain size decreased to 10 nm.[9] In this work, the average grain size of the La-STO particulate film was ca. 15 nm, and considering the porous structure of our self-assembled particulate film (relative density 78%), the low thermal conductivity, 1.5 W/mK, is considered reasonable. In spite of the enhanced phonon scattering by the grain boundaries, the electrical transport seems not to be deteriorated. Different from the conventional grain boundaries in bulk ceramics, the boundaries between nanocubes (both sides are mostly [100]-oriented) in this self-assembled particulate film could have perfect coherent interfaces, which are supposed to be beneficial for electron transport.

Motivated by the relatively high thermoelectric properties, the power generation characteristic was measured for the self-assembled particulate film of La-STO (La 5%). The $I-V$ and power density curves of the self-assembled particulate film after calcination were measured for a temperature difference of 20 K as shown in Figure 3d. The largest current density of 19.8 mA/cm^2 and voltage of 15.6 mV contributed to a maximum power density of 75 mW/cm^2. This power density is higher than that of a conventional (commercial) Bi_2Ti_3-based device (typically 37 mW/cm^2). Thus, the self-assembled film of La-STO nanocubes showed good potential for power generation near room temperature.

CONCLUSIONS

In summary, self-assembled particulate films of La-STO nanocubes with mechanically robust structure were successfully prepared for thermoelectric application. UV irradiation was used to prepare the self-assembled particulate film with a uniform structure over a large area, by in situ decomposition of the nanocube surfactants generating a mechanically robust structure. Increased phonon scattering at the nanocube interfaces lowered the thermal conductivity of the self-assembled film significantly. Consequently, we succeeded in the preparation of a self-assembled film of La-STO nanocubes with ZT values at 300 K exceeding those of single crystals. This work exemplifies the benefits of nanostructuring for enhancing thermoelectric performance of strontium titanate.

ASSOCIATED CONTENT

Supporting Information

TEM and HRTEM of La-STO nanocubes, photographs of the particulate film of La-STO nanocubes prepared without UV irradiation; FT-IR spectra, SEM images, and photograph of the self-assembled particulate film prepared under vacuum conditions; and illustration of van der Pauw method and $I-V$ curves of the self-assembled particulate film of La-nanocubes. This material is available free of charge via the Internet at http://pubs.acs.org.

AUTHOR INFORMATION

Corresponding Authors

*E-mail: feng.dang@apchem.nagoya-u.ac.jp (F.D.).
*E-mail: chunlei.wan@apchem.nagoya-u.ac.jp (C.W.).
*E-mail: koumoto@apchem.nagoya-u.ac.jp (K.K.).

Notes

The authors declare no competing financial interest.

■ ACKNOWLEDGMENTS

The authors gratefully thank Prof. Tsunehiro Takeuchi of Nagoya University for the measurement of thermal conductivity of the self-assembled particulate film.

■ REFERENCES

(1) Shanthi, N.; Sarma, D. D. *Phys. Rev. B* **1998**, *57*, 2153−2158.
(2) Kohiki, S.; Arai, M.; Yoshikawa, H.; Fukushima, S.; Oku, M.; Waseda, Y. *Phys. Rev. B* **2000**, *62*, 7964−7969.
(3) Benthem, K.; Elsässer, C.; French, R. H. *J. Appl. Phys.* **2001**, *90*, 6156−6164.
(4) Ohta, S.; Nomura, T.; Ohta, H.; Koumoto, K. *J. Appl. Phys.* **2005**, *97*, 034106-1−034106-4.
(5) Ohta, S.; Nomura, T.; Ohta, H.; Koumoto, K. *Appl. Phys. Lett.* **2005**, *87*, 092108-1−092108-3.
(6) Ohta, H.; Kim, S.-W.; Mune, Y.; Mizoguchi, T.; Nomura, K.; Ohta, S.; Nomura, T.; Nakanishi, Y.; Ikuhara, Y.; Hirano, M.; Hosono, H.; Koumoto, K. *Nat. Mater.* **2007**, *6*, 129−134.
(7) Wang, Y.; Lee, K.-H.; Hyuga, H.; Kita, H.; Inaba, K.; Ohta, H.; Koumoto, K. *Appl. Phys. Lett.* **2007**, *91*, 242102-1−242102-3.
(8) Lee, K. H.; Muna, Y.; Ohta, H.; Koumoto, K. *Appl. Phys. Express* **2008**, *1*, 015007-1−015007-3.
(9) Wang, Y. F.; Fujinami, K.; Zhang, R. Z.; Wan, C. L.; Wang, N.; Ba, Y. S.; Koumoto, K. *Appl. Phys. Express* **2010**, *3*, 031101-1−031101-3.
(10) Zhang, R. Z.; Wang, C. L.; Li, J. C.; Koumoto, K. *J. Am. Ceram. Soc.* **2010**, *93*, 1677−1681.
(11) Yamamoto, M.; Ohta, H.; Koumoto, K. *Appl. Phys. Lett.* **2007**, *90*, 072101-1−072101-3.
(12) Muta, H.; Kurosaki, K.; Yamanaka, K. *J. Alloys Compd.* **2005**, *392*, 306−309.
(13) Ravichandran, J.; Siemons, W.; Oh, D. W.; Kardel, J. T.; Chari, A.; Heijmerikx, H.; Scullin, M. L.; Majumdar, A.; Ramesh, R.; Cahill, D. G. *Phys. Rev. B* **2010**, *82*, 165126-1−165126-5.
(14) Wang, H. C.; Wang, C. L.; Su, W. B.; Liu, J.; Sun, Y.; Peng, H.; Mei, L. M. *J. Am. Ceram. Soc.* **2011**, *94*, 838−842.
(15) Scullin, M. L.; Yu, C.; Huijben, M.; Mukerjee, S.; Seidel, J.; Zhan, Q.; Moore, J.; Majumdar, A.; Ramesh, R. *Appl. Phys. Lett.* **2008**, *92*, 202113-1−202113-3.
(16) Shevchenko, E. V.; Talapin, D. V.; Kotov, N. A.; Brien, S.; Murray, C. B. *Nature* **2006**, *439*, 55−59.
(17) Li, Y. J.; Huang, W. J.; Sun, S. G. *Angew. Chem., Int. Ed.* **2006**, *45*, 2537−2539.
(18) Kurt, P.; Banerjee, D.; Cohen, R. E.; Tubner, M. F. *J. Mater. Chem.* **2009**, *19*, 8920−8927.
(19) Dang, F.; Kato, K.; Imai, H.; Wada, S.; Haneda, H.; Kuwabara, M. *Cryst. Growth Des.* **2011**, *11*, 4129−4134.
(20) Mimura, K.; Dang, F.; Kato, K.; Imai, H.; Wada, S.; Haneda, H.; Kuwabara, M. *Jpn. J. Appl. Phys.* **2011**, *50*, 09NC09-1−09NC09-6.
(21) Mimura, K.; Kato, K.; Imai, H.; Wada, S.; Haneda, H.; Kuwabara, M. *Appl. Phys. Lett.* **2012**, *101*, 012901-1−012901-4.
(22) Dang, F.; Mimura, K.; Kato, K.; Imai, H.; Wada, S.; Haneda, H.; Kuwabara, M. *CrystEngComm* **2011**, *13*, 3878−3883.
(23) Dang, F.; Mimura, K.; Kato, K.; Imai, H.; Wada, S.; Haneda, H.; Kuwabara, M. *Nanoscale* **2012**, *4*, 1344−1349.